

Low-energy total-electron-capture cross sections for fully stripped and H-like projectiles incident on H and H₂

F. W. Meyer, A. M. Howald, C. C. Havener, and R. A. Phaneuf
Oak Ridge National Laboratory, Oak Ridge, Tennessee 37831

(Received 19 June 1985)

Total-electron-capture cross sections are reported for fully stripped and H-like ions of C, N, O, F, and Ne colliding with atomic and molecular hydrogen targets in the energy range 0.18–8.5 keV/amu. At energies above 3 keV/amu the cross sections are approximately energy independent with magnitudes in the range $(4-7) \times 10^{-15}$ cm², and scale smoothly with projectile charge. Below 3 keV/amu the H-target cross sections for projectiles with even charge are smaller than those for projectiles of odd charge. For the H₂-target data, the opposite trend prevails. For those systems where calculations exist, molecular orbital and atomic orbital close-coupling calculations are within 20% of the experimental results except at the lowest energies investigated.

INTRODUCTION

Low-velocity electron-capture collisions involving multicharged ions play an important role in astrophysical¹ and fusion² plasmas, and are thus of considerable practical interest. This applied aspect of electron-capture collisions has spurred considerable theoretical effort in recent years. Particular theoretical emphasis has been given to calculations of electron capture by fully stripped projectiles colliding with atomic hydrogen. For these systems the stationary states of the quasimolecule formed during slow collisions can be accurately calculated, permitting systematic studies of the various approximations within which the transitions between these stationary states can be calculated. Experimental efforts to provide benchmark data against which to compare these calculations have lagged behind theory due to the difficulty of producing sufficient quantities of fully stripped ions to perform the required measurements. The development of a new generation of multicharged-ion sources³⁻⁵ has recently opened up this research area to experimental investigation.

Phaneuf⁶ and Phaneuf *et al.*⁷ reported total-cross-section results for electron capture by fully stripped C in collisions with H and H₂ in the energy range 0.14–0.32 keV/amu, the first such results for a fully stripped ion ($Z > 5$) in this energy range. Panov *et al.*⁸ have reported measurements of total-electron-capture cross sections for fully stripped, H-like, and He-like ions of C, N, O, Ne, and for fully stripped Ar incident on H and H₂ in the energy range 0.33–8.8 keV/amu. However, the large scatter in their H-target data precludes a meaningful comparison. Bendahman *et al.*⁹ have recently made similar measurements for fully stripped N, O, and Ne ions incident on H at a few energies in the range 1–5 keV/amu. Recent measurements of Dijkkamp *et al.*¹⁰ in the energy range 3.0–7.5 keV/amu included results of line-emission cross sections for electron-capture collisions between fully stripped C and N ions and atomic hydrogen in addition to total-cross-section results. These state-selective results provide a more stringent test of theory in the vicinity of

the peaks of the capture cross sections.

We report here on a systematic and comprehensive set of measurements of total-electron-capture cross sections for fully stripped and H-like ions of C, N, O, F, and Ne incident on atomic and molecular hydrogen in the energy range 0.18–8.5 keV/amu. The measurements were taken using a fine energy grid, and are of sufficient precision to permit meaningful comparisons with theoretical calculations over a wide energy range, including the low-energy side of the cross-section maxima where the cross sections have significant dependence on energy. The present measurements for the fully stripped ions colliding with atomic hydrogen provide important benchmark data against which to compare theoretical calculations of these one-electron systems. In addition, our results for the H-like projectiles shed light on the effect of the presence of a projectile ($1s$) core electron on the total-electron-capture cross section. Parts of this work have already been reported in a paper dealing with oscillations observed in the charge dependence of the total capture cross sections for fully stripped projectiles incident on H and H₂ at fixed collision energies below 1 keV/amu.¹¹

EXPERIMENTAL METHOD

Figure 1 shows schematically the experimental configuration used for the present measurements. Fully stripped and H-like ions of ¹³C, ¹⁵N, ¹⁸O, ¹⁹F, and ²²Ne were extracted from the Oak Ridge National Laboratory (ORNL) Electron Cyclotron Resonance (ECR) multicharged-ion source.¹² Isotopes were chosen such that the mass-per-charge ratio for the fully stripped ions was different from two, to permit magnetic separation from contaminant H₂⁺ ions. Following momentum and charge selection by a 90°, 40-cm radius-of-curvature stigmatic magnetic spectrometer, the beam traversed a collimation section that limited its divergence to ± 1.7 mrad prior to entering a 2.1 cm long target cell having 1 and 2 mm diameter entrance and exit apertures, respectively. An electrostatic parallel-plate analyzer located immediately downstream of the col-

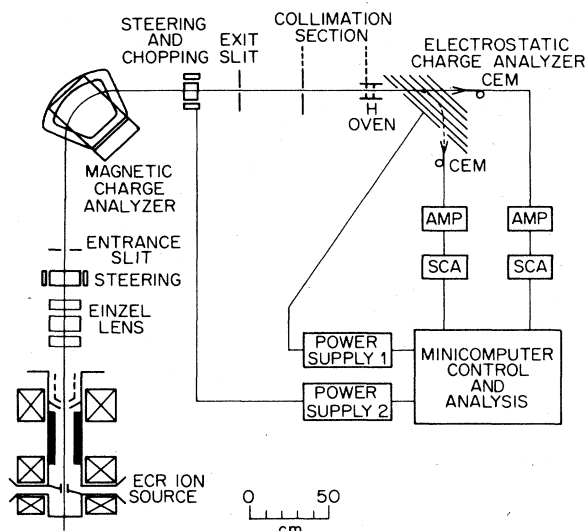


FIG. 1. Schematic diagram of the experimental setup. The straight-through CEM and the provision for beam chopping were used only during target thickness calibration.

lision target was used to alternately deflect signal ions (charge $q - 1$) and primary-beam ions (charge q) into a channel electron multiplier (CEM) operated in pulse counting mode. A microcomputer facilitated control of the experiment and data acquisition. Total-electron-capture cross sections were deduced from the fraction of signal ions produced in the collision cell at a calibrated target thickness.

By use of a guard ring situated immediately in front of the CEM and biased about 100 V more negatively than the CEM funnel, which was held typically at -3 kV, the area over which ion impacts could be detected was essentially equal to the physical cross sectional area of the funnel opening, independent of ion beam energy. Auxiliary measurements performed in our laboratory of secondary-electron emission coefficients for multicharged ions incident on a resistive glass surface similar to that found in our CEM, showed that the $3 \times q$ keV additional energy the ions acquired prior to impact as a result of the detector bias was sufficient to ensure secondary-electron emission coefficients of at least 3. Counting efficiencies were therefore at least 95%, even at the lowest energies investigated.

At all energies investigated, complete collection of ions was checked by electrostatically scanning primary and signal ions across the detector. In all cases a flat-topped response was obtained. Our experimental conclusion of complete collection of all product ions independent of collision energy is consistent with calculations by Olson and Kimura¹³ of angular scattering associated with electron-capture collisions between C^{6+} and H. This collision system is expected to have the largest angular deflection of projectile ions during capture collisions, because the projectile-target mass ratio is smallest, and because the cross sections are small at low energies. Olson and Kimura calculate for the $C^{6+} + H$ system that even at our lowest measured energy, more than 90% of the product ions will fall within our CEM acceptance angle of $\pm 1.8^\circ$.

The atomic hydrogen target was obtained by thermal dissociation of molecular hydrogen in a high-temperature tungsten oven. Details of the implementation and calibration of the hydrogen oven have been previously described.^{7,14} When cold, the oven is a standard gas cell and was used to measure electron capture in collisions with H_2 . When maintained at a typical operating temperature of 2350 K, the target consisted of $93 \pm 3\%$ atomic hydrogen. Cross sections for collisions with atomic hydrogen were determined by subtracting from the "composite" cross section measured with the oven hot the cross section measured with the oven cold weighted by the amount of H_2 remaining at 2350 K, $7 \pm 3\%$. Maximum correction to the atomic hydrogen cross sections due to undissociated H_2 was 20%, and occurred for those systems for which the H_2 target cross section exceeded the H target cross section by factors of 2–3. H_2 and H target thickness calibrations were obtained by normalization to well-established electron-capture cross sections for $H^+ + H_2$ and $H^+ + H$ at 20 keV, as has been previously described.⁷ In the course of the present measurements the H and H_2 target thickness calibrations were checked by remeasuring the above cross sections, and were found to be unchanged relative to our previous calibration.⁷ An on-axis CEM in direct view of the collision target was used during the calibration measurements to detect the H^0 collision products. For the atomic-hydrogen normalization measurement, for which the oven was hot, the beam was chopped (via power supply 2 in Fig. 1) to permit subtraction of background counts due to photons emitted by the oven tube.

In order to isolate collision events occurring in the target, i.e., to discriminate against charge changing collisions on background gas outside the target, the gas-bypass technique described by Bayfield¹⁵ was employed. Two gas feed paths of equal conductance were provided, keeping the gas load on the vacuum system constant, independent of the path used. One path led into the target cell and was used during signal measurements, while the other bypassed the cell and was used during background measurements. The target cell is differentially pumped upstream by a 1000-l/s liquid-nitrogen-trapped diffusion pump, and downstream by a cryopump having a pumping speed of 500 l/s for H_2 , which was sufficient to keep the operating pressure upstream of the target below 1×10^{-6} Torr during cross-section measurements. Typical corrections made for collisions on background gas were 30%, and were as high as 50% for the cases where the atomic hydrogen target capture cross section was much smaller than the corresponding one for background (mainly H_2) gas. Conversion fractions in the collision cell were below 10% at the target pressures used for the present measurements; corrections for double scattering of typically a few percent were made as described in the Appendix.

RESULTS AND DISCUSSION

The experimental total-electron-capture cross sections for fully stripped C, and for fully stripped and H-like N, O, F, and Ne incident on H and H_2 are summarized in Table I. The total uncertainty quoted in the table consists

TABLE I. Experimental electron-capture cross sections; total uncertainties are quoted at good confidence level (see the text).

| Ion | Energy (eV/amu) | Velocity (10^7 cm/s) | $\sigma_{q,q-1}(\text{H})$ (10^{-15} cm 2) | Total uncertainty | $\sigma_{q,q-1}(\text{H}_2)$ (10^{-15} cm 2) | Total uncertainty |
|-----------|--------------------|----------------------------|--|----------------------|--|----------------------|
| C $^{6+}$ | 230 | 2.11 | 1.30 | 0.35 | 3.90 | 0.6 |
| | 346 | 2.59 | 1.76 | 0.37 | 4.10 | 0.64 |
| | 462 | 2.98 | 2.46 | 0.41 | 4.33 | 0.68 |
| | 923 | 4.22 | 3.31 | 0.52 | 4.51 | 0.71 |
| | 1846 | 5.97 | 3.96 | 0.61 | 4.33 | 0.66 |
| | 2769 | 7.31 | 4.16 | 0.64 | 4.30 | 0.65 |
| | 3692 | 8.44 | 4.10 | 0.64 | 4.16 | 0.64 |
| | 4615 | 9.44 | 4.27 | 0.64 | 4.12 | 0.64 |
| | 5539 | 10.34 | 4.34 | 0.65 | 4.07 | 0.63 |
| | 6462 | 11.17 | 4.34 | 0.65 | 3.98 | 0.62 |
| | 7385 | 11.94 | 4.21 | 0.64 | 3.97 | 0.62 |
| | 8308 | 12.66 | 4.29 | 0.64 | 3.76 | 0.58 |
| N $^{7+}$ | 233 | 2.12 | 5.02 | 0.72 | 1.14 | 0.20 |
| | 350 | 2.60 | 4.86 | 0.71 | 1.31 | 0.23 |
| | 467 | 3.00 | 4.81 | 0.70 | 1.50 | 0.26 |
| | 700 | 3.68 | 4.69 | 0.70 | 2.03 | 0.34 |
| | 933 | 4.24 | 4.51 | 0.69 | 2.09 | 0.35 |
| | 1400 | 5.20 | 4.84 | 0.71 | 2.69 | 0.44 |
| | 1867 | 6.00 | 4.69 | 0.70 | 3.07 | 0.50 |
| | 2333 | 6.71 | 4.79 | 0.71 | 3.27 | 0.53 |
| | 3500 | 8.22 | 4.94 | 0.72 | 3.74 | 0.61 |
| | 4667 | 9.49 | 4.92 | 0.72 | 3.87 | 0.63 |
| | 6533 | 11.23 | 5.04 | 0.72 | 4.27 | 0.69 |
| | 8167 | 12.55 | 4.94 | 0.72 | 4.25 | 0.69 |
| N $^{6+}$ | 214 | 2.03 | 2.30 | 0.39 | 3.83 | 0.64 |
| | 321 | 2.49 | 2.77 | 0.44 | 4.27 | 0.69 |
| | 429 | 2.88 | 3.17 | 0.51 | 4.49 | 0.69 |
| | 643 | 3.52 | 3.41 | 0.57 | 4.55 | 0.77 |
| | 857 | 4.07 | 3.31 | 0.56 | 4.48 | 0.76 |
| | 1286 | 4.98 | 3.51 | 0.58 | 4.37 | 0.74 |
| | 1714 | 5.75 | 3.73 | 0.63 | 4.34 | 0.74 |
| | 2000 | 6.21 | 3.85 | 0.64 | 4.34 | 0.74 |
| | 2142 | 6.43 | | | 4.20 | 0.71 |
| | 3000 | 7.61 | 3.88 | 0.64 | 4.11 | 0.69 |
| | 4826 | 9.09 | 4.17 | 0.71 | 4.16 | 0.70 |
| | 6000 | 10.76 | 4.27 | 0.72 | 4.11 | 0.69 |
| 7500 | 12.03 | 4.20 | 0.72 | 3.97 | 0.67 | |
| O $^{8+}$ | 178 | 1.85 | 1.41 | 0.36 | 2.92 | 0.50 |
| | 222 | 2.07 | 2.24 | 0.36 | 4.22 | 0.70 |
| | 333 | 2.53 | 2.88 | 0.46 | 4.73 | 0.74 |
| | 444 | 2.93 | 3.42 | 0.54 | 4.98 | 0.78 |
| | 667 | 3.59 | 4.04 | 0.63 | 5.16 | 0.81 |
| | 889 | 4.14 | 4.48 | 0.70 | 5.27 | 0.83 |
| | 1333 | 5.07 | 5.27 | 0.82 | 5.23 | 0.82 |
| | 1778 | 5.86 | 5.38 | 0.84 | 5.14 | 0.81 |
| | 2222 | 6.55 | 5.43 | 0.85 | 5.01 | 0.79 |
| | 3333 | 8.02 | 5.51 | 0.85 | 4.91 | 0.78 |
| | 4444 | 9.26 | 5.61 | 0.88 | 4.92 | 0.78 |
| | 6222 | 10.96 | 5.78 | 0.89 | 5.02 | 0.79 |
| 8000 | 12.42 | 5.50 | 0.85 | 4.85 | 0.76 | |
| O $^{7+}$ | 175 | 1.84 | 4.76 | 0.88 | 1.17 | 0.34 |
| | 219 | 2.06 | 4.92 | 0.78 | 1.88 | 0.43 |
| | 328 | 2.52 | 5.14 | 0.81 | 1.71 | 0.27 |

TABLE I. (Continued).

| Ion | Energy (eV/amu) | Velocity (10^7 cm/s) | $\sigma_{q,q-1}(\text{H})$ (10^{-15} cm 2) | Total uncertainty | $\sigma_{q,q-1}(\text{H}_2)$ (10^{-15} cm 2) | Total uncertainty |
|------------------------------|--------------------|----------------------------|--|----------------------|--|----------------------|
| | 438 | 2.91 | 5.08 | 0.80 | 1.82 | 0.47 |
| | 656 | 3.56 | 4.77 | 0.75 | 2.24 | 0.35 |
| | 875 | 4.11 | 4.78 | 0.75 | 2.57 | 0.40 |
| | 1313 | 5.03 | 5.14 | 0.81 | 3.03 | 0.48 |
| | 1750 | 5.81 | 5.03 | 0.78 | 3.31 | 0.52 |
| | 2188 | 6.50 | 4.96 | 0.77 | 3.49 | 0.55 |
| | 3281 | 7.96 | 4.80 | 0.75 | 3.70 | 0.58 |
| | 4375 | 9.19 | 4.87 | 0.76 | 3.89 | 0.61 |
| | 6125 | 10.87 | 4.84 | 0.76 | 4.12 | 0.65 |
| | 7875 | 12.33 | 5.04 | 0.78 | 4.22 | 0.66 |
| F$^{9+}$ | 379 | 2.70 | 7.36 | 1.33 | 3.58 | 0.64 |
| | 474 | 3.02 | 6.73 | 1.21 | 3.66 | 0.66 |
| | 592 | 3.38 | 6.66 | 1.20 | | |
| | 711 | 3.70 | 6.29 | 1.13 | 4.13 | 0.74 |
| | 947 | 4.27 | 6.57 | 1.18 | 4.25 | 0.77 |
| | 1184 | 4.78 | 6.89 | 1.24 | | |
| | 1421 | 5.24 | 6.77 | 1.22 | 4.80 | 0.86 |
| | 1705 | 5.74 | 6.51 | 1.17 | | |
| | 1990 | 6.20 | 6.66 | 1.20 | | |
| | 2386 | 6.76 | 6.29 | 1.13 | 5.12 | 0.92 |
| | 3553 | 8.28 | 6.75 | 1.22 | 5.51 | 1.00 |
| | 4737 | 9.56 | 6.97 | 1.25 | 5.71 | 1.03 |
| | 6632 | 11.31 | 7.16 | 1.29 | 6.07 | 1.09 |
| | 8526 | 12.83 | 6.69 | 1.20 | 6.02 | 1.08 |
| F$^{8+}$ | 421 | 2.85 | 3.96 | 0.67 | 5.51 | 0.93 |
| | 632 | 3.49 | 4.51 | 0.76 | 5.64 | 0.95 |
| | 842 | 4.03 | 4.66 | 0.78 | 5.51 | 0.93 |
| | 1263 | 4.94 | 5.05 | 0.85 | 5.61 | 0.94 |
| | 2105 | 6.37 | 5.15 | 0.87 | 5.57 | 0.94 |
| | 3158 | 7.81 | 5.54 | 0.93 | 5.35 | 0.90 |
| | 4211 | 9.01 | 5.91 | 1.00 | 5.38 | 0.89 |
| | 5895 | 10.67 | 5.98 | 1.00 | 5.27 | 0.88 |
| | 7579 | 12.09 | 5.99 | 1.01 | 5.32 | 0.89 |
| Ne$^{10+}$ | 909 | 4.19 | 6.36 | 1.15 | 6.38 | 0.95 |
| | 1364 | 5.13 | 7.03 | 1.27 | 6.54 | 1.33 |
| | 2273 | 6.62 | 6.84 | 1.04 | 6.01 | 0.90 |
| | 2773 | 7.32 | 7.08 | 1.08 | 5.96 | 0.90 |
| | 3409 | 8.11 | 7.20 | 1.10 | 6.10 | 0.92 |
| | 4545 | 9.37 | 7.02 | 1.07 | 6.07 | 0.92 |
| | 6364 | 11.08 | 7.16 | 1.09 | 6.01 | 0.91 |
| | 8182 | 12.57 | 7.07 | 1.08 | 5.92 | 0.89 |
| Ne$^{9+}$ | 205 | 1.99 | 7.33 | 0.99 | 3.56 | 0.64 |
| | 307 | 2.43 | 6.73 | 1.28 | 3.70 | 0.64 |
| | 409 | 2.81 | 6.74 | 1.14 | 4.06 | 0.70 |
| | 614 | 3.44 | 6.71 | 1.13 | 4.39 | 0.76 |
| | 818 | 3.97 | 6.70 | 1.06 | 4.61 | 0.74 |
| | 1227 | 4.87 | 6.67 | 1.05 | 4.90 | 0.77 |
| | 2045 | 6.28 | 6.63 | 1.08 | 5.08 | 0.95 |
| | 3068 | 7.69 | 6.68 | 1.06 | 5.51 | 0.86 |
| | 4091 | 8.89 | 6.47 | 1.08 | 5.55 | 0.94 |
| | 5727 | 10.51 | 6.57 | 1.10 | 5.69 | 0.93 |
| | 7364 | 11.92 | 6.77 | 1.35 | 5.56 | 0.90 |

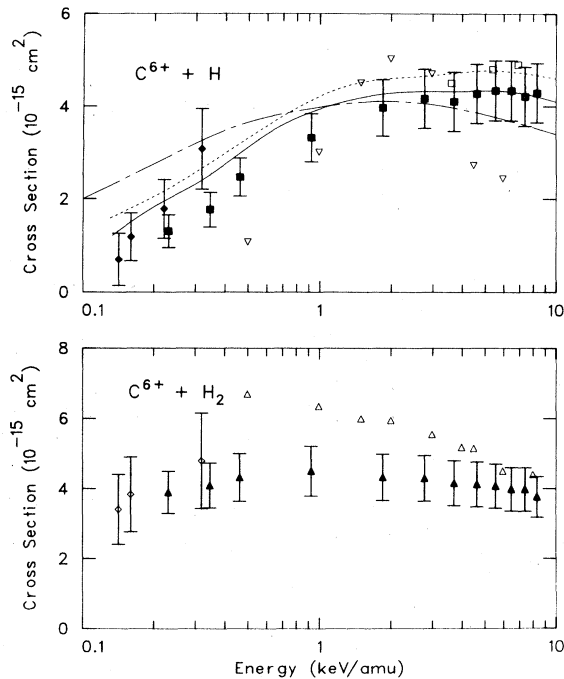


FIG. 2. Total electron-capture cross sections for C^{6+} ions incident on H and H_2 . ■ and ▲, present results; ◆ and ◇, measurements of Phaneuf *et al.* (Ref. 7); ▽ and △, data of Panov *et al.* (Ref. 8); □, data of Dijkkamp *et al.* (Ref. 10); —, (AO) expansion calculation by Fritsch and Lin (Ref. 18); - - -, (MO) expansion calculation by Green *et al.* (Ref. 17); - · - ·, MLZRC calculation by Janev *et al.* (Ref. 19). Error bars on present data represent total absolute experimental uncertainty at "good confidence" level (see the text).

of an absolute systematic uncertainty of 13.5% as described previously¹⁶ summed in quadrature with a relative uncertainty of typically 8–12% (though higher for some of the lower energy data points). The relative uncertainty was estimated from the larger of either counting statistics or repeated measurements of certain points (usually on different days). Both systematic and relative uncertainties were estimated at "good confidence," intended to be equivalent to 90% confidence level on statistics. Total uncertainty associated with a cross-section measurement is typically $\pm 17\%$ at this level. In Figs. 2–6 the present results are graphically summarized and compared with other measurements as well as theoretical calculations.

C^{6+} projectiles

Figure 2 shows the present results for C^{6+} incident on H and H_2 . For both the atomic and molecular hydrogen target data the present data join smoothly with the less precise low-energy results of Phaneuf *et al.*⁷ Atomic hydrogen target measurements of Dijkkamp *et al.*¹⁰ at 3.6, 5.4, and 6.9 keV/amu are in excellent agreement with the present results. The data of Panov *et al.*⁸ for molecular hydrogen are characterized by a steeper energy dependence than our results, and agree with the present mea-

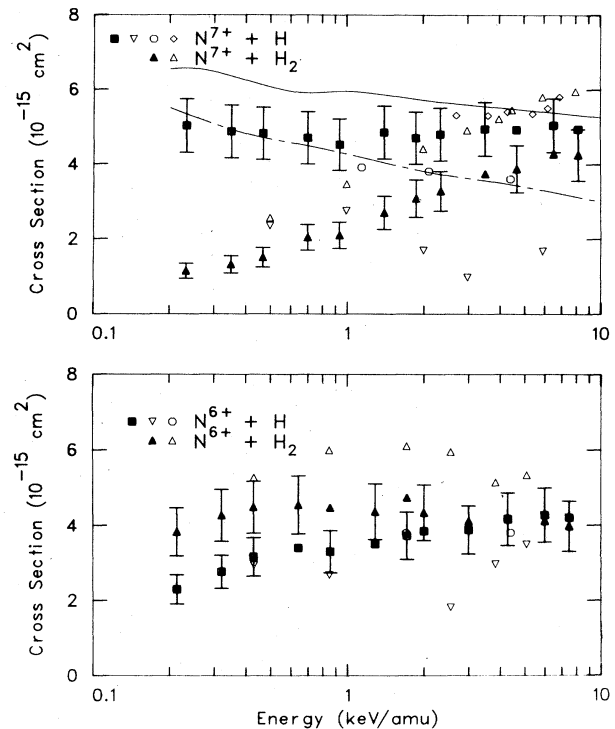


FIG. 3. Total-electron-capture cross sections for N^{7+} and N^{6+} ions incident on H and H_2 . ○, data of Bendahman *et al.* (Ref. 9); remaining symbols and curves defined as in Fig. 2, except for open diamonds, which here are data of Dijkkamp *et al.* (Ref. 10). Some error bars omitted from the present data to avoid cluttering.

surements only above ~ 5 keV/amu, falling above our results by as much as 50% at lower energies. The atomic hydrogen data of Panov *et al.* are also shown in Fig. 2, as well as in subsequent figures, despite the large scatter that makes comparison difficult. The large scatter in the H target data of Panov *et al.* is believed to be due partly to the large corrections required in their measurements as a result of a low effective dissociation fraction ($\sim 35\%$).

Also shown in Fig. 2 is a 33-state molecular orbital (MO) perturbed-stationary-state calculation by Green *et al.*,¹⁷ which lies slightly above the present experimental results above 2 keV/amu, but still within the experimental uncertainty of the measurements. Below 2 keV/amu, the calculation of Green *et al.* does not fall with decreasing energy as steeply as the present results, and lies $\sim 50\%$ higher than the present data at the lowest energy measured. A calculation by Fritsch and Lin¹⁸ based on a 35-state atomic orbital (AO) expansion also is in very good agreement with the present results at energies above 1 keV/amu, and lies in magnitude between the calculation of Green *et al.* and our experimental results. Also shown in Fig. 2 is a multichannel Landau-Zener with rotational coupling (MLZRC) calculation by Janev *et al.*¹⁹ The inclusion of rotational coupling has the effect of slightly shifting the calculated cross-section maximum to lower energies and of increasing the magnitude of the cross sec-

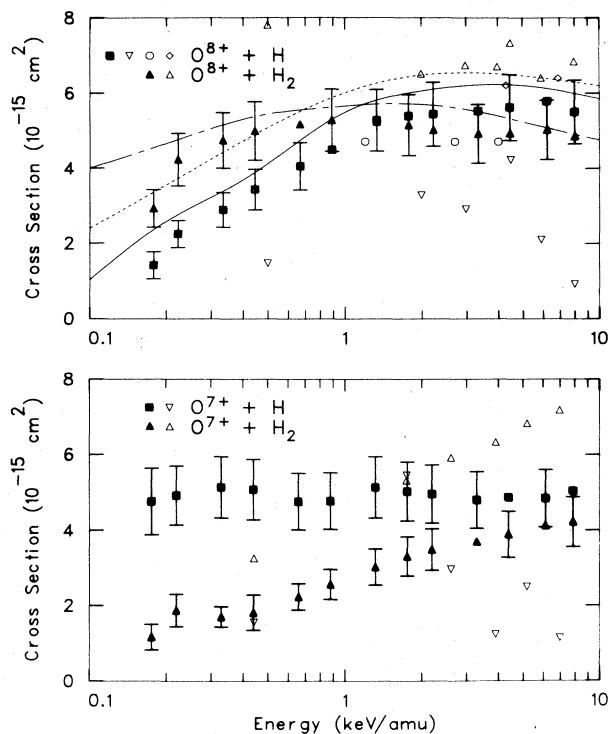


FIG. 4. Total-electron-capture cross sections for O^{8+} and O^{7+} ions incident on H and H_2 . Symbols and curves defined as in Fig. 2, except for the open diamonds, which here are data of Dijkkamp *et al.* (Ref. 10); and dashed curve, which here is the 33-state (MO) calculation by Shipsey *et al.* (Ref. 20). Some error bars omitted from present data to avoid cluttering.

tion in the energy region below the maximum relative to the usual Landau-Zener model, and brings the calculation into surprisingly good accord with the present measurements. Additional calculations of the $C^{6+} + H$ system exist (see Refs. 9, 17, 19, and 20 and references therein); the calculations explicitly referred to in the above comparison are illustrative of three different theoretical approaches, and are all believed to be converged with respect to the size of the basis sets used.

N^{6+}, N^{7+} projectiles

Figure 3 shows the present measurements for N^{6+} and N^{7+} projectiles colliding with H and H_2 . As can be seen from the figure, the measurements of Bendahman⁹ *et al.* for the $N^{7+} + H$ system are in reasonable accord with the present results, falling 15–30% below our data but still within combined experimental uncertainties of the two measurements. The results of Dijkkamp *et al.* for the same collision system in the range 2.7 to 6.9 keV/amu are in excellent accord with the present results. The results of Bendahman *et al.* for the $N^{6+} + H$ system at 1.7 and 4.4 keV/amu lie within 10% of the present data for this system. For both the N^{7+} and N^{6+} projectiles incident on H_2 , the measurements of Panov *et al.* lie above the present results by 20–50%. The atomic hydrogen target results of Panov *et al.* are shown for completeness only, as discussed in the previous section.

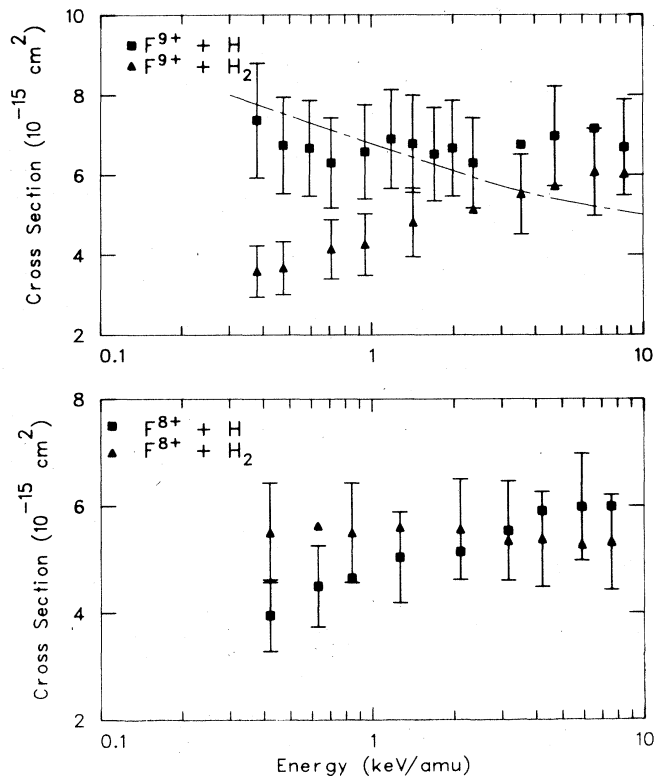


FIG. 5. Total-electron-capture cross sections for F^{9+} and F^{8+} ions incident on H and H_2 . Symbols and curves defined as in Fig. 2. Some error bars omitted from present data to avoid cluttering.

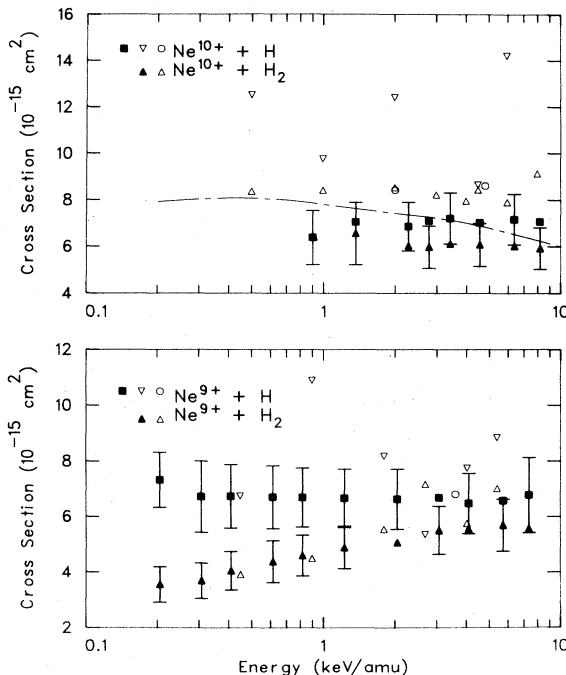


FIG. 6. Total-electron-capture cross sections for Ne^{10+} and Ne^{9+} ions incident on H and H_2 . Symbols and curves defined as in Figs. 2 and 3. Some error bars omitted from present data to avoid cluttering.

Included in Fig. 3 are an AO close-coupling calculation by Fritsch and Lin and a MLZRC calculation by Janev *et al.*, both for the $N^{7+} + H$ system. The AO calculation is in reasonable agreement with the present measurements above 3 keV/amu, while tending to overestimate the cross section by up to 30% at the lowest measured energy. The MLZRC calculation falls 30–60% below the AO curve and is in very good agreement with the present results below 1 keV/amu. The excellent accord between the five-state molecular orbital expansion calculation of Ref. 9, not shown in Fig. 3, and the present data may be fortuitous, since their restricted basis size probably leads to an underestimation of the total capture cross section.

O^{7+}, O^{8+} projectiles

The present results for O^{7+} and O^{8+} projectiles incident on H and H_2 are shown in Fig. 4. In the case of the $O^{8+} + H$ system, both the measurements of Bendahman in the energy range 1.2–4.0 keV/amu, and the measurements of Dijkamp *et al.* at 4.3 and 6.9 keV/amu are within experimental uncertainty of the present results. The molecular hydrogen target results of Panov *et al.* for O^{7+} and O^{8+} projectiles lie about 75% and 25% above the present measurements, respectively. Again, the H target results of Panov *et al.* are shown for completeness; see the comments in the C^{6+} section.

For the $O^{8+} + H$ system, Fig. 4 also shows theoretical results of a 33-state MO perturbed stationary state calculation by Shipsey *et al.*,²⁰ an AO close-coupling calculation by Fritsch and Lin, and a MLZRC calculation from Ref. 19. As was the case in the $C^{6+} + H$ system, the AO calculation is in best accord with the present results, agreeing with the measurements to within experimental uncertainty at all but the lowest two energies. The MO calculation lies above the AO results, and thus is characterized by a larger discrepancy relative to our measurements, of typically 20% above 1 keV/amu, and of as much as a factor of 2 at the lowest energies. The MLZRC calculation overestimates the experimental results of low energies by more than a factor of 2, but is in excellent agreement with experiment above 1 keV/amu. The five-state MO calculation in Ref. 9, not shown in the figure, gives results indistinguishable from those of Fritsch and Lin below 1 keV/amu, while lying slightly below (by less than 10%) the latter results in the energy range 1–10 keV/amu, presumably because of the smaller basis set used.

F^{8+}, F^{9+} projectiles

Figure 5 summarizes the present results for F^{8+} and F^{9+} projectiles incident on H and H_2 . We are aware of no other measurements for either of these systems with which to compare the present results. The only calculations for the $F^{9+} + H$ system are believed to be the MLZRC calculation of Ref. 19, which, despite a slightly different energy dependence, is in reasonable accord with the present measurements; and the seven-state molecular orbital expansion calculation of Ref. 9, which lies within 10% of the present measurements over the whole energy range investigated.

Ne^{9+}, Ne^{10+} projectiles

The present results for Ne^{9+} and Ne^{10+} ions are shown in Fig. 6. The cross-section data for the $Ne^{10+} + H$ system at 2.0 and 4.8 keV/amu by Bendahman *et al.*, also shown in the figure, lie $\sim 20\%$ above the present measurements, yet still within the combined experimental uncertainties. The measurement for the $Ne^{9+} + H$ system by Bendahman *et al.* at 3.6 keV/amu is in excellent agreement with the present results for that system. In the case of the H_2 results of Panov *et al.*, their cross-section results are in excellent agreement with the present measurements of the $Ne^{9+} + H$ system, and about 35% above our values in the case of the $Ne^{10+} + H$ system. As was the case with the other H target data of Panov *et al.*, their data for Ne^{9+} and Ne^{10+} projectiles are scattered widely, and thus have a poorly defined energy dependence and mean magnitude. The only calculations of the $Ne^{10+} + H$ capture cross section are believed to be the MLZRC result from Ref. 19 and the seven-state MO calculation of Ref. 9, not shown in Fig. 6. Again agreement with the present results in the energy range investigated is good in the case of the MLZRC results, even though, as was already noted for the $F^{9+} + H$ system, the calculation has a slightly stronger energy dependence than the present measurements. The molecular orbital calculation in Ref. 9 reproduces very well the present measurements of the $Ne^{10+} + H$ system below 3 keV/amu, while falling slightly below the present results at higher energies (by up to 10% at 8 keV/amu).

Projectile core effect

Figure 7 shows a comparison between our measured total capture cross sections for fully stripped ions and for H-like ions having the same charge, at two different collision energies. It may be seen from the figure that the cross-section magnitude depends primarily on the ionic charge, and is rather insensitive to the presence of the (1s) core electron in the H-like projectiles. The relative insensitivity of the total capture cross section to the presence or number of core electrons has been previously observed by Crandall *et al.*¹⁶ when comparing He-like and Li-like ions of charge 3–6 incident on H and H_2 , by Bliman *et al.*²¹ for fully stripped and H-like ions of charge 3–7 incident on H_2 , and by Iwai *et al.*²² when comparing fully stripped, H-like and He-like ions of charge 5–8 incident on He. For all the above systems, capture is expected to occur into excited states having principal quantum number, i.e., $n \geq 3$.^{18,24,25} It is reasonable that the level structure and binding energies of these highly excited states should be only weakly influenced by a tightly bound core, due to the small spatial overlap of the core and excited electrons. The energies of these excited levels, therefore, depend to a first approximation only on ionic charge. Since at the collision energies investigated in the present measurements the final excited state level structure is the prime determinant of the electron-capture cross section,^{26,27} the cross sections themselves should also only depend on ionic charge. This point is illustrated very nicely in the work of Gordeev *et al.*,²³ who measured cross sections for electron capture into particular nl states during

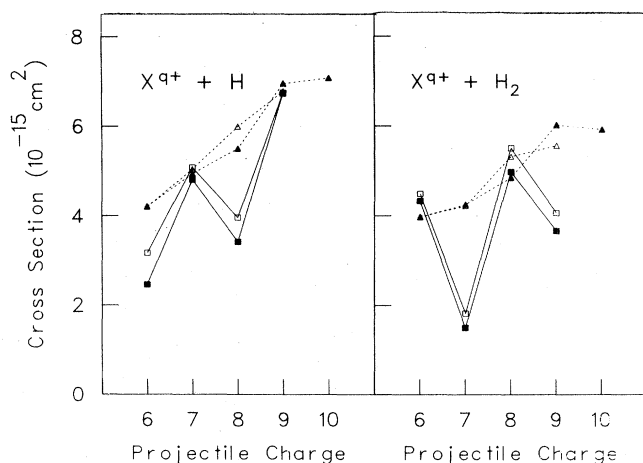


FIG. 7. Comparison of experimental electron-capture cross sections for fully stripped projectiles (solid symbols) and H-like projectiles (open symbols) incident on H and H₂ targets; triangles and dashed lines—7.5 keV/amu collision energy; squares and solid lines—0.45 keV/amu collision energy.

low energy collisions of C⁶⁺, N⁶⁺, and O⁶⁺ incident on He, and found that, as long as the populated *nl* levels have hydrogenlike binding energies, the influence of the ionic core on the capture process is small, i.e., the σ_{nl} 's depend only on *q*.

Oscillations in *q* dependence

Figure 8 shows in greater detail the charge scaling of the total capture cross sections for the fully stripped projectiles at several different fixed collision energies. As may be seen from the figure, at energies below 3 keV/amu, the cross sections for both atomic and molecular hydrogen are characterized by an oscillatory dependence on projectile charge. In the case of the atomic hydrogen target data, cross sections for projectiles having even charge are smaller (by up to a factor of 3 at the

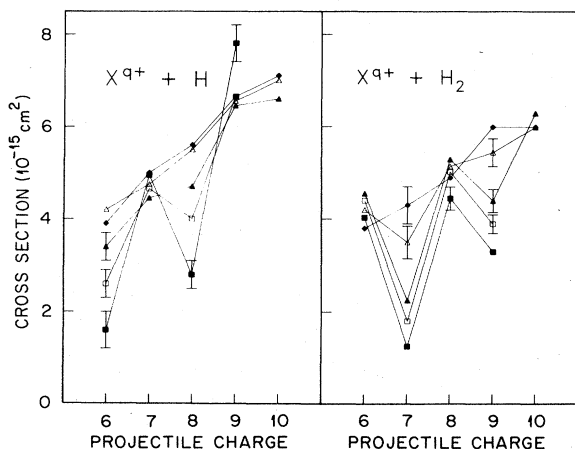


FIG. 8. Charge dependence of experimental total-electron-capture cross sections for fully stripped projectiles ($6 \leq Z \leq 10$) incident on H and H₂. ■, 0.3 keV/amu; □, 0.6 keV/amu; ▲, 1.0 keV/amu; △, 3.0 keV/amu; ◆, 8.0 keV/amu. A few representative error bars are indicated.

lowest energy) than those for projectiles of odd charge. For the molecular hydrogen target data, the opposite trend prevails. As the collision velocity is increased from 0.3 keV/amu, the above patterns in the charge scaling persist; however, the deviations from a purely monotonic charge dependence of the cross sections become progressively smaller. At energies of 3 keV/amu and higher, the oscillations are no longer apparent, the cross sections being characterized instead by a more or less smooth dependence on projectile charge.

The observed oscillatory dependence of the total-electron-capture cross sections on projectile charge is attributed to the extreme state selectivity of the capture collision at low velocities, and has been predicted theoretically.^{9,19,27} The oscillatory charge dependence observed in the present collision systems and its interpretation in terms of a simple Landau-Zener model has been discussed in a separate publication.¹¹

SUMMARY

Total-electron-capture cross sections have been measured for fully stripped and H-like ions of C, N, O, F, and Ne colliding with atomic and molecular hydrogen in the energy range 0.18–8.5 keV/amu. Both the measurements of Bendahman *et al.* for the N⁶⁺, N⁷⁺, O⁸⁺, Ne⁹⁺, and Ne¹⁰⁺+H systems and the results of Dijkamp *et al.* for the C⁶⁺, N⁷⁺, and O⁸⁺+H systems are in very good agreement with the present measurements, the maximum discrepancy in all cases being less than the combined experimental uncertainties of the two measurements ($\approx 30\%$). As regards comparison with theory, both the AO and MO calculations reproduce the measured cross sections extremely well (to better than 20%) above 2 keV/amu where the cross sections have little energy dependence. At energies below 2 keV/amu, where the energy dependence is more pronounced, both calculations tend to overestimate the measured cross sections, due either to a weaker predicted energy dependence in those cases (C⁶⁺, O⁸⁺+H) where the cross sections fall with decreasing energy below 2 keV/amu, or a slightly stronger energy dependence in the N⁷⁺+H case where the measured cross section rises slightly below 2 keV/amu. Maximum disagreement for the AO calculation is $\approx 40\%$ (C⁶⁺+H) and about a factor of 2 (O⁸⁺+H) for the MO calculation, both occurring at the lowest energies measured. The MLZRC calculation gives a surprisingly good estimate of the capture cross section at energies above 1 keV/amu, but significantly overestimates the C⁶⁺, O⁸⁺+H cross sections below 1 keV/amu where there is significant energy dependence.

ACKNOWLEDGMENTS

This work was sponsored by the Division of Chemical Sciences, U.S. Department of Energy, under Contract No. DE-AC05-84OR21400 with Martin Marietta Energy Systems, Inc. The ORNL ECR multicharged ion source was developed with the support of the Office of Fusion Energy, U.S. Department of Energy. A.M.H. and C.C.H. were

appointed through the U.S. Department of Energy Post-graduate Research Training Program administered by Oak Ridge Associated Universities.

APPENDIX

Consider a projectile beam of charge i incident on a gas target of thickness π . According to Allison,²⁸ the fraction of ions of charge $i-1$ emerging from the target is given, in a three-component approximation, by

$$F_{i-1} = F_{i-1}^{\infty} + [P(i, i-1)\exp(\pi q) + N(i, i-1)\exp(-\pi q)] \exp\left[-\frac{1}{2}\pi \sum \sigma_{if}\right], \quad (\text{A1})$$

where

$$P(i, i-1) = \frac{1}{2q} [F_{i-1}^{\infty}(s-q) - bF_{i-2}^{\infty}]$$

and

$$N(i, i-1) = -\frac{1}{2q} [F_{i-1}^{\infty}(s+q) - bF_{i-2}^{\infty}],$$

F_{i-1}^{∞} and F_{i-2}^{∞} are the equilibrium fractions for charge states $i-1$ and $i-2$, respectively; and s , q , b , and $\sum \sigma_{if}$ are different combinations of the various cross sections through which the three components are coupled, as defined in Ref. 28. At the energies investigated in the

present experiment, electron capture is the dominant charge changing collision, i.e., stripping collisions can be neglected.²⁹ The following simplification results in Eq. (A1) when all the stripping cross sections are set to zero,

$$F_{i-1} = \frac{\sigma_{i,i-1}}{q} \sinh(\pi q) \exp\left[-\frac{1}{2}\pi \sum \sigma_{if}\right] \quad (\text{A2})$$

since $F_{i-1}^{\infty} = 0$, $F_{i-2}^{\infty} = 1$, and $b \sim -\sigma_{i,i-1}$ in the absence of stripping. When Eq. (A2) is expanded in powers of the target thickness, and only linear and quadratic terms in π are retained, one obtains

$$F_{i-1} \approx \pi \sigma_{i,i-1} \left[1 - \frac{1}{2}\pi \sum \sigma_{if}\right], \quad (\text{A3})$$

where

$$\sum \sigma_{if} = \sigma_{i,i-1} + \sigma_{i,i-2} + \sigma_{i-1,i-2}.$$

Solving for $\sigma_{i,i-1}$, and making the assumption that $\pi \sum \sigma_{if} \ll 1$, one obtains

$$\sigma_{i,i-1} \cong \frac{F_{i-1}}{\pi} \left[1 + \frac{1}{2}\pi \sum \sigma_{if}\right]. \quad (\text{A4})$$

Provided that stripping can be neglected, the double scattering correction applied to the experimentally determined fraction F_{i-1} is thus seen to be the factor $(1 + \frac{1}{2}\pi \sum \sigma_{if})$, where $\sum \sigma_{if}$ is the sum of all single and multiple electron-capture cross sections that deplete either primary or signal beams.

¹See, e.g., A. Dalgarno, in *Invited Papers of the XII International Conference on the Physics of Electronic and Atomic Collisions, Gatlinburg, 1981*, edited by S. Datz (North-Holland, Amsterdam, 1982), p. 1.

²See, e.g., J. T. Hogan, in Ref. 1, p. 769.

³E. D. Donets, *Phys. Scr.* **T3**, 11 (1983).

⁴R. Geller, B. Jacquot, and R. Pauthenet, *Rev. Phys. Appl.* **15**, 995 (1980).

⁵R. A. Phaneuf, *IEEE Trans. Nucl. Sci.* **NS-28**, 1182 (1981).

⁶R. A. Phaneuf, *Phys. Rev. A* **24**, 1138 (1981).

⁷R. A. Phaneuf, I. Alvarez, F. W. Meyer, and D. H. Crandall, *Phys. Rev. A* **26**, 1892 (1982).

⁸M. N. Panov, A. A. Basalae, and K. O. Lozhkin, *Phys. Scr.* **T3**, 124 (1983).

⁹M. Bendahman, S. Bliman, S. Dousson, D. Hitz, R. Gayet, J. Hanssen, C. Harel, and A. Salin, *J. Phys. (Paris)* **46**, 561 (1985).

¹⁰D. Dijkkamp, D. Ćirić, and F. J. de Heer, *Phys. Rev. Lett.* **54**, 1004 (1985).

¹¹F. W. Meyer, A. M. Howald, C. C. Havener, and R. A. Phaneuf, *Phys. Rev. Lett.* **53**, 2663 (1985).

¹²F. W. Meyer, *Proceedings of the International Conference on the Physics of Highly Ionized Ions, Oxford, 1984* [*Nucl. Instrum. Methods* **B9**, 532 (1985)].

¹³R. E. Olson and M. Kimura, *J. Phys. B* **15**, 4231 (1982).

¹⁴R. A. Phaneuf, F. W. Meyer, and R. H. McKnight, *Phys. Rev. A* **17**, 534 (1978).

¹⁵J. E. Bayfield, *Phys. Rev.* **182**, 1156 (1969).

¹⁶D. H. Crandall, R. A. Phaneuf, and F. W. Meyer, *Phys. Rev. A* **19**, 504 (1979).

¹⁷T. A. Green, E. J. Shipsey, and J. C. Browne, *Phys. Rev. A* **25**, 1364 (1982).

¹⁸W. Fritsch and C. D. Lin, *Phys. Rev. A* **29**, 3039 (1984).

¹⁹R. K. Janev, D. C. Belić, and B. H. Brandsen, *Phys. Rev. A* **28**, 1293 (1983).

²⁰E. J. Shipsey, T. A. Green, and J. C. Browne, *Phys. Rev. A* **27**, 821 (1983).

²¹S. Bliman, J. Aubert, R. Geller, B. Jacquot, and D. Van Houtte, *Phys. Rev. A* **23**, 1703 (1981).

²²T. Iwai, Y. Kaneko, M. Kimura, N. Kobayashi, S. Ohtani, K. Okuno, S. Takagi, H. Tawara, and S. Tsurubuchi, *Phys. Rev. A* **26**, 105 (1982).

²³Yu. S. Gordeev, D. Dijkkamp, A. G. Drentje, and F. J. de Heer, *Phys. Rev. Lett.* **50**, 1842 (1983).

²⁴M. Kimura, T. Iwai, Y. Kaneko, N. Kobayashi, A. Matsumoto, S. Ohtani, K. Okuno, S. Takagi, H. Tawara, S. Tsurubuchi, *J. Phys. Soc. Jpn.* **53**, 2224 (1984).

²⁵O. G. Larsen and K. Taulbjerg, *J. Phys. B* **17**, 4523 (1984).

²⁶R. K. Janev, *Phys. Scr.* **T3**, 208 (1983).

²⁷H. Ryufuku, K. Sasaki, and T. Watanabe, *Phys. Rev. A* **21**, 745 (1980).

²⁸S. K. Allison, *Rev. Mod. Phys.* **30**, 1137 (1958).

²⁹S. Bliman, N. Chang-Tung, S. Dousson, B. Jacquot, and D. Van Houtte, *Phys. Rev. A* **21**, 1856 (1980).